International Conference on Military Technologies (ICMT) 2019
May 30 – 31, 2019, Brno, Czech Republic

Internal Ballistics of High-Low Pressure Decoy Launcher with a Secondary Propellant Charge

Dung Nguyen Thai[1], Vladimír Horák[2], Linh Do Duc[1], and Hong Nguyen Lac[1]
[1] Le Quy Don Technical University, Bac Tu Liem District, Hanoi, Vietnam,
e-mail: *thaidung1996@gmail.com,* e-mail*: duclinh.do@gmail.com,* e-mail*: bihe65@yahoo.com*
[2] Department of Mechanical Engineering, University of Defence, Kounicova 65, Brno, Czech Republic,
e-mail: *vladimir.horak@unob.cz*

***Abstract*—This paper presents a novel concept of a naval decoy launcher working on the principle of high-low pressure system using a secondary propellant charge located in the low-pressure chamber. A system of internal ballistic equations suitable for computer analysis is developed to predict the considered decoy launcher performance. The problem is solved using MATLAB environment. The variation of gases pressure and the time change of decoy velocity and displacement are studied. An experimental setup has been established for the purpose of verifying the results of solution.**

Keywords-high-low pressure; internal ballistics; decoy; decoy launcher; high-low

NOMENCLATURE

ψ	Relative burnt propellant mass
z	Relative burnt thickness of grain
κ, λ, μ	Form function coefficients
φ	Coefficient of fictivity
α	Covolume of propellant gases
I_k	Total impulse of propellant gases
f	Specific energy of propellant (force)
χ	Geometric characteristics of powder grain
ω	Propellant charge mass
W_0	Chamber initial volume
v	Decoy velocity
l	Decoy displacement
m	Decoy mass

Subscripts:

1	High-pressure chamber
2	Low-pressure chamber
12	From high- to low-pressure chamber

I. INTRODUCTION

One of engineering challenges in designing decoy launching systems is that of increasing the range of fire while the recoil forces are kept low.

The high-low pressure system is a common design of anti-tank and grenade launchers, that use a smaller high-pressure chamber in order to store the propellant. The weapons class utilizing the high-low pressure system achieves some major advantages as bellow [1]:

- The weapon can be designed with a reduced or negligible recoil.
- Much larger projectile to be launched without the heavy equipment typically required for large caliber weapons.
- The weight of the weapon and its ammunition can be significantly reduced.
- Manufacturing cost and production time are substantially lower than for standard weapon systems firing a projectile of the same caliber and weight.
- More efficient use of the propellant, unlike earlier recoilless weapons, where most of the propellant is expended to the rear of the weapon to counter the recoil of the projectile being fired.

The only major drawback of high-low pressure systems is its maximum range of fire. Hence, the essential idea is of using the high-low pressure system with a secondary propellant located in the low-pressure chamber. There is almost no available literature on the internal ballistics of such weapon system. There are several related publications documenting the internal ballistics of weapon utilizing the high-low pressure system [2], [3].

This study is a theoretical and experimental analysis of the internal ballistics of the decoy launchers used in surface ships. The goal of the study is to investigate the various physical processes involved in the firing of the decoy launcher utilizing the high-low pressure system with the secondary propellant located in the low-pressure chamber. For the purpose of

978-1-7281-4593-8/19/$31.00

experimental verification of the developed mathematical internal ballistic model an experimental setup has been established.

The concept presented in this paper is believed to be an improvement over the design of existing decoy launchers mounted in many surface warships, such as the Russian PK-2, -10, and -16 decoy dispense systems.

II. Principle of Operation of the Presented Decoy Launcher

The new concept of the decoy launcher is shown in Fig. 1.

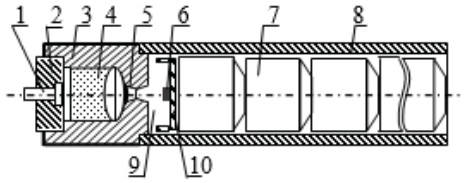

Figure 1. Schematic of the decoy launcher concept: 1- Primer; 2- Breechblock; 3- High-pressure chamber; 4- Basic propellant charge; 5- Nozzle; 6- Secondary propellant charge; 7- Decoy; 8- Launcher tube; 9- Low-pressure chamber; 10- Piston.

As shown in the above figure, the decoy launcher is consisting of the high-pressure chamber 3 and the low-pressure chamber 9. The high- and low-pressure chamber are connected through the nozzle 5. The propellant charges 4 and 6 located in the high- and low-pressure chamber are referred to as the basic charge, and secondary charge, respectively.

The internal ballistic cycle starts with the ignition of basic propellant charge 4 that burns in the constant high-pressure chamber volume until the moment when the propellant gas pressure achieves the value at which the propellant charge covering and additional liner plate that seal the nozzle rupture. When the nozzle 5 is opened, the hot generated gases discharge from the high-pressure chamber 3 into the low-pressure chamber 9, where they ignite the secondary propellant charge located under the piston 10. The decoy 7 consisting of six modules starts moving, when the shot-start gas pressure is reached in the low-pressure chamber.

The internal ballistics duration of presented decoy launcher can be divided into three periods:

- The 1st period is considered from the burning of basic propellant charge until when the shot-start pressure is reached in the low-pressure chamber or when the decoy starts moving in the launcher tube.
- The 2nd period is from when the decoy starts moving until the moment when the propellant burning is completed (i.e. all-burnt point) within the launcher tube.
- The 3rd period is from the all-burnt until the decoy has left the launcher muzzle.

III. Mathematical Model

A. Asumptions

The internal ballistic mathematical model is developed on the basis of the following major assumptions:

- The propellant charge burns in accordance with geometrical law of powder propellant burning. The burning rate is a function of the gas pressure.
- The influences of physical phenomena taking place inside the low-pressure chamber on the combustion of the basic propellant charge within the high-pressure chamber and the gas discharge throw the nozzle are negligible.
- Heat loss to the chambers surface can be accounted for adequately by applying an adjustment factor reducing the available energy released by the burning propellant.
- The propellant charge is immediately ignited and then burns simultaneously. The propellant ignition is assumed isochoric. There is no unburnt basic propellant discharged into the low-pressure chamber.
- The decoy consisting of six modules is considered as a single rigid body. The propellant burning and decoy motion is caused by the average gas pressure within each chambers.
- The flow in the high-pressure chamber is quasi-steady. There are no pressure waves or gradients introduced into the system.
- One-dimensional flow of heterogeneous gas mixture through the nozzle.
- The gas pressure reached at the all-burnt point inside the high-pressure chamber is the maximum pressure.
- The gas flow through the nozzle is isentropic. The gas temperature in the high-pressure chamber is smaller than the propellant combustion temperature.

B. Equations of Mathematical Model

1) High-pressure chamber

a) Propellant burning

The equations describing propellant burning taking place in the high-pressure chamber can be set based on the usual internal ballistic assumptions [4]:

$$\frac{\mathrm{d}z_1}{\mathrm{d}t} = \frac{p_1}{I_{k1}} \tag{1}$$

$$\frac{\mathrm{d}\psi_1}{\mathrm{d}t} = \chi_1(1 + 2\lambda z_1 + 3\mu z_1)\frac{\mathrm{d}z_1}{\mathrm{d}t} \tag{2}$$

b) Gas flow rate though the nozzle

The time change in quantity of the discharge gas through the nozzle is given by [5]

$$\frac{\mathrm{d}\eta_1}{\mathrm{d}t} = \frac{\mu_{12} K_0 S_{th}}{\omega_1 \sqrt{\chi_{n1} f_1 \tau_1}} (p_1 - p_2) \tag{3}$$

Where: η_1 is the quantity of the outflow gas, S_{th} accounts for the nozzle critical area, μ_{12} denotes the discharge coefficient, ω_1 is the mass of basic propellant charge, and τ_1 is the relative temperature defined as the ratio of the high-pressure chamber temperature T_1 to the basic propellant combustion temperature T_c, thus

$$\tau_1 = \frac{T_1}{T_c} \tag{4}$$

The coefficient K_0 appearing in Eq. (3) is given by

$$K_0 = \left(\frac{2}{\kappa+1}\right)^{\frac{\kappa+1}{2(\kappa-1)}} \sqrt{g\kappa} \tag{5}$$

Where κ is the specific heat ratio.

c) Equation of state

The equation of state within the high-pressure chamber can be written in the form as [6]:

$$p_1 = \frac{f_1 \tau_1 \omega_1 (\psi_1 - \eta_1)}{W_{0,1} - \frac{\omega_1}{\delta_1}(1-\psi_1) - \alpha_1 \omega_1 (\psi_1 - \eta_1)} \tag{6}$$

d) Equation of energy

Then, the equation of energy can be written in the form as bellow [5]

$$\frac{\mathrm{d}\tau_1}{\mathrm{d}t} = \frac{(1-\tau_1)\frac{\mathrm{d}\psi_1}{dt} + (1-\kappa)\tau_1 \frac{\mathrm{d}\eta_1}{dt}}{\psi_1 - \eta_1} \tag{7}$$

2) Low-pressure chamber

a) Propellant burning

The equations describing propellant burning in the low-pressure chamber is given by [4]:

$$\frac{\mathrm{d}z_2}{\mathrm{d}t} = \frac{\mathrm{d}_2}{I_{k2}} \tag{8}$$

$$\frac{\mathrm{d}\psi_2}{\mathrm{d}t} = \chi_2 (1 + 2\lambda z_2 + 3\mu z_2) \frac{\mathrm{d}z_2}{\mathrm{d}t} \tag{9}$$

b) Gas flow rate

In this investigation, the gas flow through the gap between the decoy outer diameter and the launcher tube inner diameter is taken into consideration. The time change in quantity of the outflow gas through this gap is given by [5]

$$\frac{\mathrm{d}\eta_2}{\mathrm{d}t} = \frac{\mu_{2a} K_o S_{kh}}{\omega \sqrt{\chi_{n2} f^* \tau_2}} (p_2 - p_a) \tag{10}$$

Where: η_2 is the quantity of the outflow gas, S_{kh} denotes the cross-sectional gap area, μ_{2a} denotes the discharge coefficient, ω is the summation of the basic and secondary mass.

The relative temperature τ_2 is defined as the ratio of the low-pressure chamber temperature T_2 to the secondary propellant combustion temperature T_c, thus

$$\tau_2 = \frac{T_2}{T_c} \tag{11}$$

c) Equation of state

If we take the gas flow through the gap between the decoy outer diameter and the launcher tube inner diameter into consideration, then the equation of state for the low-pressure chamber can be given in form:

$$p_2 = \frac{f^* \tau_2 (\omega_1 \eta_1 + \omega_2 \psi_2 - \omega \eta_2)}{\mathrm{W}_{0,2} - \alpha_2 (\omega_1 \eta_1 + \omega_2 \psi_2 - \omega \eta_2) - \frac{\omega_2}{\delta_2}(1-\psi_2) + S_n l} \tag{12}$$

Where $\omega_1 \eta_1$ represents for the amount of gas discharged from the high-low pressure chamber, $\omega_2 \psi_2$ accounts for the amount of burnt gas of the secondary propellant charge, and $\omega \eta_2$ is the amount of gas escaping through the gap mentioned above.

The equivalent specific energy of the propellant is defined as

$$f^* = \frac{f_1 \omega_1 + 0.5 f_2 \omega_2}{\omega_1 + 0.5 \omega_2} \tag{13}$$

Where f_1 and f_2 represent for the specific energy of the basic and secondary propellant charge, respectively.

d) Equation of energy

Next, we derive the equation of energy for the low-pressure chamber. Applying the law of conservation of energy for the low-pressure chamber we obtain

$$\mathrm{d}Q = \mathrm{d}U + \mathrm{d}W \tag{14}$$

The left side of Eq. (14) represents the quantity of energy added to the low-pressure chamber that is summation of the energy $\mathrm{d}Q_1$ and $\mathrm{d}Q_2$.

Where:

- The energy $\mathrm{d}Q_1$ caused by the inlet gas flow from the high-pressure chamber is given as

$$\mathrm{d}Q_1 = \frac{\kappa R}{\kappa - 1} T_1 \omega_1 \mathrm{d}\eta_1 \tag{15}$$

- The change in energy $\mathrm{d}Q_2$. due to the combustion of the secondary propellant charge can be calculated as

$$\mathrm{d}Q_2 = \omega_2 C_V T_1 \mathrm{d}\psi_2 \tag{16}$$

The right side of Eq. (14) expresses the change in the internal energy of the system $\mathrm{d}U$ and the total quantity of energy losses $\mathrm{d}W$ due to work done.

The change in the internal energy $\mathrm{d}U$ of the low-pressure chamber is given by the change in mass of gas $\mathrm{d}Q_3$ and the change in system temperature $\mathrm{d}Q_4$. Then $\mathrm{d}U$ can be expressed as

$$\mathrm{d}U = \mathrm{d}Q_3 + \mathrm{d}Q_4 \tag{17}$$

$$\mathrm{d}U = \begin{bmatrix} C_V T_2(\omega_1 \mathrm{d}\eta_1 + \omega_2 \mathrm{d}\psi_2 - \omega \mathrm{d}\eta_2) \\ +C_V(\omega_1\eta_1 + \omega_2\psi_2 - \omega\eta_2)\mathrm{d}T_2 \end{bmatrix} \tag{18}$$

The quantity of energy loses $\mathrm{d}W$ is given by

$$\mathrm{d}W = \mathrm{d}Q_5 + \mathrm{d}Q_6 \tag{19}$$

Where:

- the energy loss $\mathrm{d}Q_4$ due to the gas escape through the gap between the decoy and barrel bore is calculated by the formula

$$\mathrm{d}Q_5 = \frac{\kappa R}{\kappa - 1} T_1 \omega \mathrm{d}\eta_2 \tag{20}$$

- the energy loss $\mathrm{d}Q_6$ to accelerate the decoy and for other works done in the system can be expressed as

$$\mathrm{d}Q_6 = \varphi m v \mathrm{d}v \tag{21}$$

By introducing Eqs. (20) and (21) into Eq. (19), then introducing Eqs. (15), (16), (18) and (19) into Eq. (14) and by rearranging we obtain

$$\frac{\mathrm{d}\tau_2}{\mathrm{d}t} = \frac{1}{\omega_1\eta_1 + \omega_2\psi_2 - \omega\eta_2} \begin{bmatrix} (\kappa\tau_1 - \tau_2)\omega_1 \dfrac{\mathrm{d}\eta_1}{\mathrm{d}t} - \omega\tau_2 \dfrac{\mathrm{d}\eta_2}{\mathrm{d}t} \\ +(1-\tau_2)\omega_2 \dfrac{\mathrm{d}\psi_2}{\mathrm{d}t} - \dfrac{\theta m}{f^*}\varphi v \dfrac{\mathrm{d}v}{\mathrm{d}t} \end{bmatrix} \tag{22}$$

3) Equations of the decoy motion

Finally, to close the system of equations, the equation of motion of the decoy are setup as bellow

$$\frac{\mathrm{d}l}{\mathrm{d}t} = v \tag{23}$$

$$\frac{\mathrm{d}v}{\mathrm{d}t} = \frac{S_n p_2}{\varphi m} \tag{24}$$

IV. Model Validation and Varification

The developed internal ballistic model of the presented decoy launcher consists of the following equations describing:

- The propellant burning in chamber: Equations (1), (2), (8) and (9).
- The gas flows: Equations (3) and (10).
- The change in chambers temperature: Equations (7) and (22).
- The decoy motion: Equations (23) and (24).
- Change in chambers pressure: Equations (6) and (12).

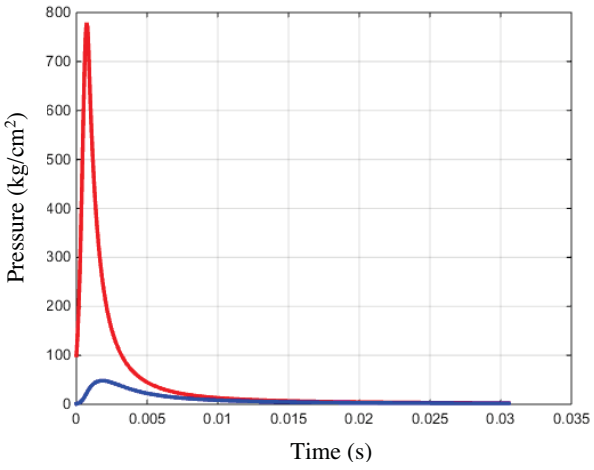

Figure 2. Time curves of pressure in high-pressure (red) and low-pressure (blue) chamber.

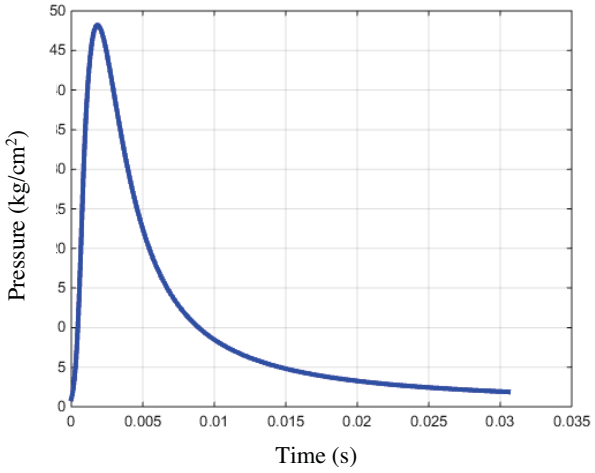

Figure 3. Time curve of pressure in the low-pressure chamber.

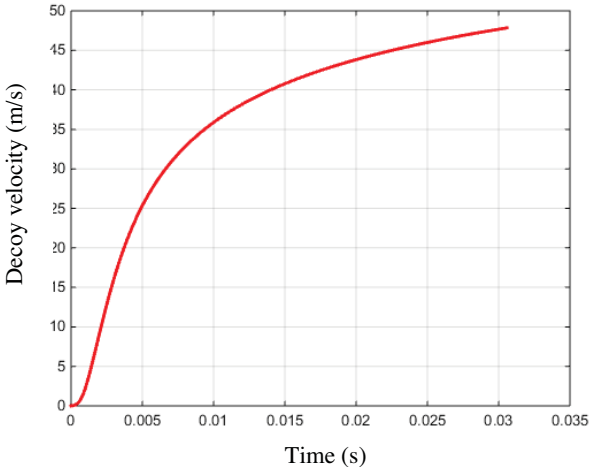

Figure 4. The decoy velocity vs. time.

TABLE I DESIGN PARAMETERS OF THE PRESENTED DECOY LAUNCHER SYSTEM

Parameters	Signification	Value	Parameters	Signification	Value
Caliber (m)	D	0.11	Chamber propellant charge mass (kg)	ω_1	0.00392
Length of decoy launcher (m)	L	1.1096		ω_2	0.0049
Cross-sectional area of launcher tube bore (m^2)	S_n	0.0095	Specific energy of propellant (J/kg)	f_1	$0.85\text{x}10^6$
Cross-sectional critical nozzle area (m^2)	S_{th}	$3.14\text{x}10^{-5}$		f_2	$1.02\text{x}10^6$
Nozzle titl angle (rad)	θ_n	0.3	Covolume of powder gas (m^3/kg)	$\alpha_1 = \alpha_2$	$0.84\text{x}10^{-3}$
Chamber initial volume (m^3)	$W_{0,1}$	$1.539\text{x}10^{-5}$	Total pressure impulse of propellant gases (Pa.s)	I_{k1}	$0.472\text{x}10^6$
				I_{k2}	$4.738\text{x}10^6$
	$W_{0,2}$	$29.148\text{x}10^{-5}$	Loading density (kg/m^3)	$\Delta_1 = \Delta_2$	$1.6\text{x}10^{-6}$
Decoy mass (kg)	m	8.8	Geometric characteristics of powder grain	χ_1	1.2
				χ_2	0.72
Specific heat ratio	κ	1.2	Surrounding pressure (Pa)	P_a	10^5

The above system of internal ballistic equations is applied for the decoy launcher system, whose design parameters are shown in Tab. 1.

The results of solution are clearly shown in Fig. 2, Fig. 3 and Fig. 4.

V. EXPERIEMTAL VERIFICATION

For the purpose of verifying the mathematical model measurements on the prototype of the decoy launcher system based on the concept shown in Fig. 1 are performed.

In the first phase of experimental part based on the available devices for experimental implementation, we choose the indirect method in order to satisfy the goal of verifying the developed mathematical model. The chosen indirect method is based on comparison of the calculated muzzle decoy velocity to the value approximated from measured data.

In order to measure the pellet velocity, we use the high-speed camera FASTCAM SA1.1 model 675K - C1, that is located 30 m to the launcher system to record the movement of the decoy, the chosen record rate was 1000 frames per second. Then, the decoy velocity is computed using video analysis that is based on the decoy movement in a set time period. The video analysis was performed automatically using a computer software from the camera provider. The video imagery of a firing test on the prototype can be seen in Fig. 5.

The calculated and measured decoy muzzle velocity values are compared in Tab. 2., from that we can conclude quite good agreement between the results of the mathematical model and experimentally obtained values.

TABLE II DECOY VELOCITY COMPARISON

Parameters	Model	Experiment	Difference
Decoy velocity (m/s)	47.84	45.16	5.6 %

Figure 5. Video imagery of firing test on the prototype of the decoy launcher.

VI. CONCLUSION

In this paper, the internal ballistic mathematical model of the naval decoy launcher working on the principle of high-low pressure system using a secondary propellant charge located in the low-pressure chamber is formulated. The problem is solved in MATLAB environment.

The model was partially verified by comparing the muzzle decoy velocity with measured data. The model fits the data quite well.

In the second phase of experimental verification the time courses of pressures within the decoy launcher chambers will be measured in order to comprehensively verify the accuracy of the developed mathematical model. Then, sensitivity analysis of the presented model could be also taken into consideration.

ACKNOWLEDGMENT

The work presented in this paper has been supported by the specific research project of Faculty of the Military Technology SV18-216, University of Defence in Brno.

REFERENCES

[1] High-low system, [online] [cited 2019-02-28], available from: < https://en.wikipedia.org/wiki/High%E2%80%93low_system>.

[2] T. Vasile, D. Safta, C. Barbu, "Studies and researchers concerning grenade launcher with high-low pressure chambers", [online] [cited 2019-02-26], available from: <https://www.researchgate.net/publication /267238161_Studies_and_researchers_concerning_grenade_launcher_with_high-low_pressure_chambers>.

[3] J. N. Kapur, The internal ballistics of a recoil-less high-low pressure gun, "Applied Scientific Research", vol. 6, issue 5-6, , 1957, p. 445-466.

[4] B. Plíhal, S. Beer, and L. Jedlička. "Interior ballistics of barrel weapons" (in Czech). Brno: University of Defence, 2004. ISBN 80-85960-83-4. 350 p.

[5] Phạm Văn Luận, "Analysis of rocket engine working on the high-low pressure principle", [Ph.D Thesis], Vietnam, Hanoi: Military Technical Academy, 2013.

[6] S. Jaramaz, D. Mickovi´c, Z. Zivkovi´c and R.´ Curci´c, **"***Internal ballistic principle of high/low pressure chambers in automatic grenade launchers",* 19th International Symposium of Ballistics, 7–11 May 2001, Interlaken, Switzerland.